The Effect of Heat Input on the Microstructure and Properties of C-Mn All-Weld-Metal Deposits

The optimum Mn level for maintaining impact properties remains at 1.4% regardless of heat input

BY G. M. EVANS

SYNOPSIS. The effect of varying the heat input, between 0.6 and 4.3 kJ/mm, on the microstructure and properties of manual metal arc deposits containing 0.6–1.8% Mn has been investigated.

It was found that an increased bead size was accompanied by a decrease in the amount of acicular ferrite and a general coarsening of the microstructure. The tensile properties were reduced on increasing the heat input, and optimum impact properties were achieved at approximately 2 kJ/mm.

The significance of the impact results is discussed in terms of the degree of recrystallization and the location of the notch.

Introduction

The present investigation is part of a continuing program (Ref. 1-3) to evaluate the factors affecting the properties of manual metal arc welds and deals with the effect of heat input on ISO 2560 type weldments as prepared for routine classification of electrodes.

A range of heat inputs was achieved by varying the electrode run out length and introducing weaving so as to yield deposits having different numbers of passes per layer. Two previously investigated factors – namely, interpass temperature (Ref. 2) and electrode diameter (Ref. 3) – were standardized.

Experimental Procedure

Electrodes

Four batches of experimental iron powder type basic electrodes (coded A, B, C and D) were prepared as for the previous investigations (Ref. 1-3). The ferromanganese contents of the coatings were varied so as to yield deposits containing 0.6, 1.0, 1.4 and 1.8 % Mn, respectively. The core wire diameter was 4 mm (0.16 in.), and the coating factor (D/d) was 1.70.

Weld Preparation

Four test series were conducted, the nominal energy inputs being 0.6, 1.0, 2.2 and 4.3 kJ/mm.

The weld preparation was that specified in ISO 2560; 4, 3, 2 and 1 beads were deposited per layer. To accommodate the different number of runs, the root opening was set at 20, 18, 16 and 14 mm (0.79, 0.71, 0.63 and 0.55 in.), respectively. The plates were buttered, and welding was done in the flat position using DC (electrode positive). The interpass temperature was maintained at 200° C (392°F) and the respective cooling times, between 800 and 500° C (1472 and 932°F), were determined at the French Welding Institute to be 4, 7, 13, and 34 seconds (s). The welding conditions, for the range extending from the fine stringer bead to the fully weaved condition, are given in Table 1.

Mechanical Testing

Two subsize all-weld-metal tensile specimens (Minitrac) were machined and tested for each electrode type and welding sequence. Also approximately 35 Charpy-V notch specimens were struck in each case to obtain complete transition curves. The impact specimens were in the as-welded condition; on the other hand, the tensile specimens were given a hydrogen removal treatment at 250° C (482°F) for 14 hours (h).

Table 1—Welding Details

Beads/ layer	Layers	Run-out length,[a] mm	Amperage, A	Voltage, V	Speed, mm/s	Heat-input, kJ/mm
4	12	660	170	22	6.18	0.6
3	9	400	170	22	3.58	1.0
2	6	200	170	22	1.66	2.2
1	6	100	170	22	0.87	4.3

(a) ~ for 410 mm of electrode. Also, 1 in. = 25.4 mm.

Results

Chemical Composition

The chemical analyses of the all-weld metal deposits are given in Table 2. A tendency existed for the carbon, manganese and silicon levels to decrease with increasing heat input.

Metallographic Examination

General. Transverse sections of multi-run deposits, having 4, 3, 2 and 1 beads per layer, are shown in Fig. 1. It can be seen that the plates had been buttered and that the root opening had been modified to accommodate the different number of passes. A 2% nital etch was employed, and that composition B (1% Mn) gave the best visual impression of the manner of build-up of the weldments.

Measurements on the last deposited bead, in each case, revealed that nugget cross-sectional areas and the supercritically heat-affected zone (HAZ) increased linearly with increasing heat input – Fig. 2. The band widths, in the vertical midplane position, were measured as in previous work (Ref. 1-3), and the resultant diagram for electrode B is given in Fig. 3. The bands became wider with increasing heat input, and the degree of recrystallization differed along the center line dependent on the number of beads per layer.

Paper to be presented on the Professional Program of the 63rd Annual AWS Convention in Kansas City, Missouri, during April 25-30, 1982.

G. M. EVANS is with Welding Industries Oerlikon Buehrle Ltd., Zurich, Switzerland.

Table 2—Chemical Compositions and Tensile Data for Deposits Welded at Different Heat Inputs

Heat input, kJ/mm	Electrode	Composition, % C	Mn	Si	S	P	σ_E, N/mm²	σ_R, N/mm²	El.,[a] %	R.A.,[b] %
0.6	A	0.044	0.62	0.32	0.007	0.007	445	496	31.0	79.7
	B	0.046	0.96	0.31	0.008	0.012	479	527	27.8	77.0
	C	0.050	1.42	0.38	0.007	0.009	511	575	26.8	78.7
	D	0.055	1.93	0.35	0.007	0.011	587	633	24.2	76.9
1.0	A	0.037	0.60	0.29	0.006	0.009	401	466	32.0	81.5
	B	0.039	0.94	0.29	0.007	0.011	438	501	32.6	80.6
	C	0.048	1.41	0.35	0.006	0.012	479	551	29.8	78.8
	D	0.051	1.80	0.32	0.006	0.012	507	587	29.2	76.9
2.2	A	0.038	0.55	0.24	0.007	0.005	389	457	30.0	80.6
	B	0.036	0.89	0.24	0.008	0.010	400	478	32.6	80.6
	C	0.042	1.37	0.28	0.007	0.012	438	518	29.8	82.3
	D	0.045	1.69	0.26	0.007	0.012	456	548	32.0	78.8
4.3	A	0.043	0.52	0.20	0.009	0.010	341	453	32.6	78.8
	B	0.042	0.93	0.20	0.008	0.011	376	484	32.6	78.8
	C	0.043	1.37	0.24	0.008	0.013	405	500	31.8	80.6
	D	0.047	1.73	0.25	0.007	0.014	437	541	30.0	78.8

(a) El.—elongation.
(b) R.A.—reduction in area.

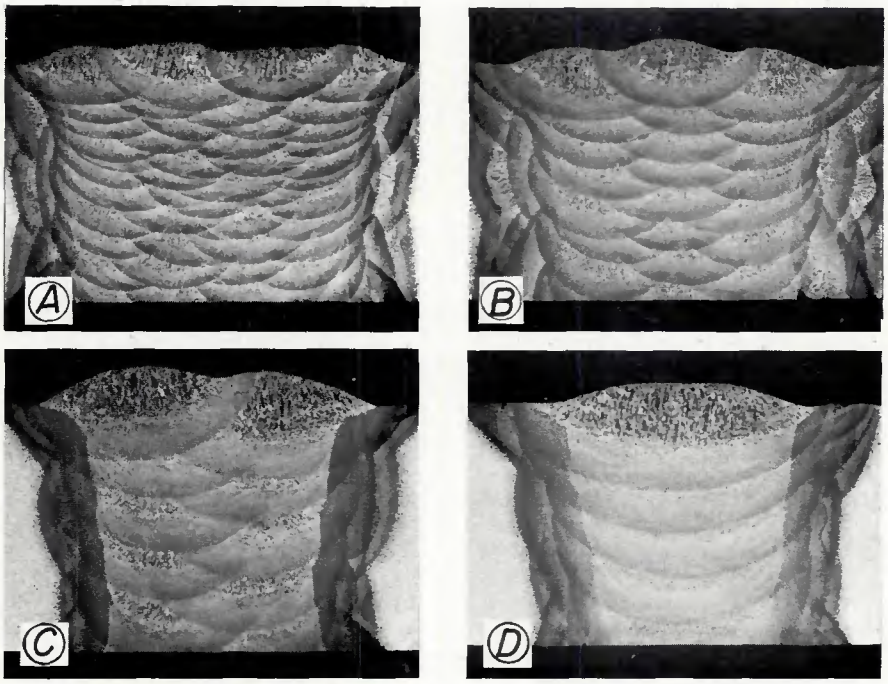

Fig. 1—Cross sections of multi-run deposits made with different heat inputs: A—0.6 kJ/mm; B—1.0 kJ/mm; C—2.2 kJ/mm; D—4.3 kJ/mm X2.5 (reduced 37% on reproduction)

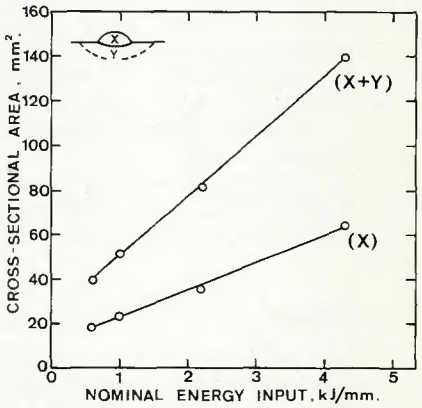

Fig. 2—Effect of heat input on nugget and recrystallized areas

The extent of recrystallization was studied in detail by comparing the manner of overlapping in the central part of weldments deposited at 1.0 and 2.3 kJ/mm. The zonal distribution for a three pass per layer weld is shown, individually and summarized, as a function of distance from the center-line in Fig. 4. A bi-modal distribution is apparent, the central position, (i.e., the Charpy-V notch location) being 75% recrystallized. The equivalent graphs for a two pass per layer weld are presented in Fig. 5 and show complete recrystallization at the center with a high degree of columnarity at locations further removed. For the fully weaved deposits (4.3 kJ/mm), the HAZ's penetrated to such an extent that no columnar structure remained in the mid-section.

Hardness traverses (HV 5) along the center line of a normal stringer (1.0 kJ/mm) and a fully weaved (4.3 kJ/mm) deposit are shown in Fig. 6. A wave distribution is apparent for the former, the peaks tending to coincide with the unrefined columnar regions. Lower hardnesses were encountered for the high heat input deposit; it can be noted that a minimum occurred in the fine grained region directly below the top bead (Ref. 3).

As-Deposited Weld Metal. Examination of as-deposited weld metal at low magnification revealed that the width of the columnar grains increased as the heat input was increased. The effect is quantified in Fig. 7 and is more pronounced than in previous work (Ref. 3), since a greater range of heat inputs was achieved by weaving than by changing the electrode diameter.

The last bead to be deposited on each weldment was examined at X200, and quantitative metallographic measurements (Ref. 4-5) were made to identify the three major microstructural components, namely:

1. Pro-eutectoid ferrite.
2. Bainite (ferrite side plates).
3. Acicular ferrite.

The point count results are given in Fig. 8; they reconfirm (Ref. 1-3) once again the role of manganese. An increase in heat input had a measurable but limited effect on the percentage. The micro-

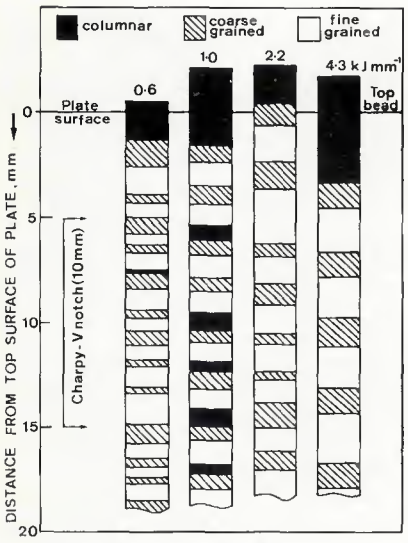

Fig. 3 — Zone distribution along vertical center line (electrode B, different heat inputs)

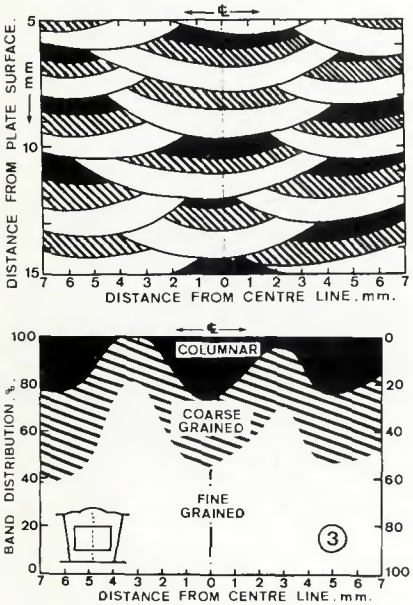

Fig. 4 — Actual and summarized zonal distribution at the center of a three pass per layer weldment

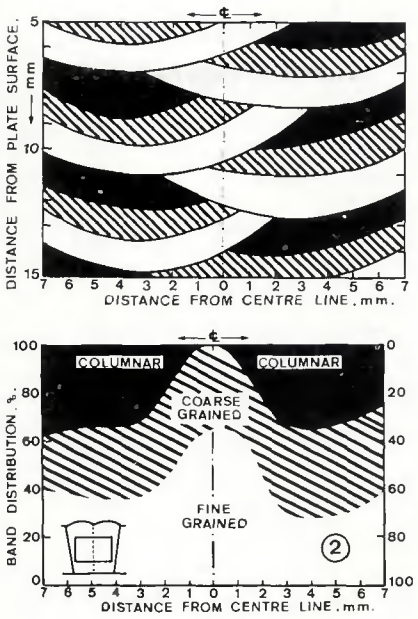

Fig. 5 — Actual and summarized zonal distribution at the center of a two pass per layer weldment

structure, however, coarsened considerably, the ferrite ribbons becoming wider (Fig. 9) with the concurrent increase in the width of the columnar grains. Also, the lath size of the acicular ferrite increased, as shown in Fig. 10, when comparing the two extremes encountered.

Hardness results obtained for the top bead in each case are given in Table 3. The relatively high interpass temperature employed (Ref. 2), i.e., 200° C (392°F), led to low hardness values throughout and to only a moderate change on varying the heat input.

Reheated weld metal. Examination of the coarse grained regions directly below the last beads to be deposited revealed that the ferrite grains delineating the prior austenite grain boundaries became larger as the heat input was increased. The effect is illustrated, for composition C by the photomicrographs shown in Fig. 11. Of note is the fact that the acicular microstructure within the ferrite envelopes coarsened and that a ferrite side plate structure appeared. The width of the apparent coarse grained region logically increased as the heat input was increased.

Examination of the fine grained regions revealed that the grain size increased with increasing heat input, as exemplified in Fig. 12 for composition C at the two extremes studied. For 0.6 kJ/mm the grains were duplex in character, whereas for the fully weaved deposits the cooling rates were retarded to such an extent that pearlite commenced to form. Linear intercepts of grain boundaries were made at X630, and the reciprocal of the square root of the mean grain interval is plotted in Fig. 13, for weld metals A and C, as a function of heat input. Non-linear relationships were obtained as also was the case when plotting the grain size factor against the yield strength of the deposits — Fig. 14.

Mechanical Properties

Tensile Results. Tensile test results are presented in Table 2. The yield strengths and the ultimate tensile strengths are plotted against weld metal manganese content in Figs. 15 and 16, respectively. Both tensile parameters decreased substantially on increasing the heat input, the drop on changing the latter from 0.6 to 4.3 kJ/mm being on average approximately 100 N/mm2 at the intermediate manganese level.

On assuming the tensile properties to be linearly related to manganese, the

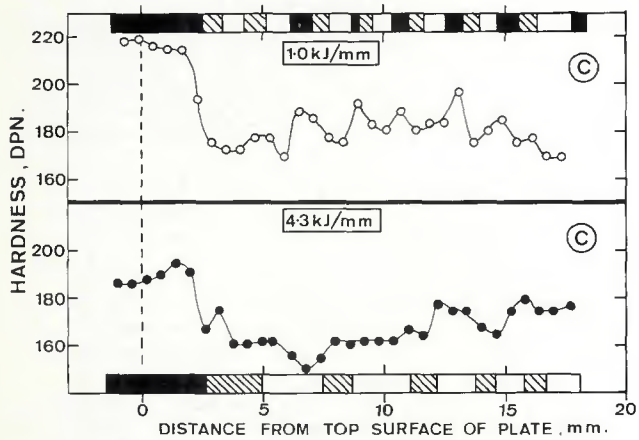

Fig. 6 — Hardness traverse along the vertical center line (electrode C, 1.0 and 4.3 kJ/mm)

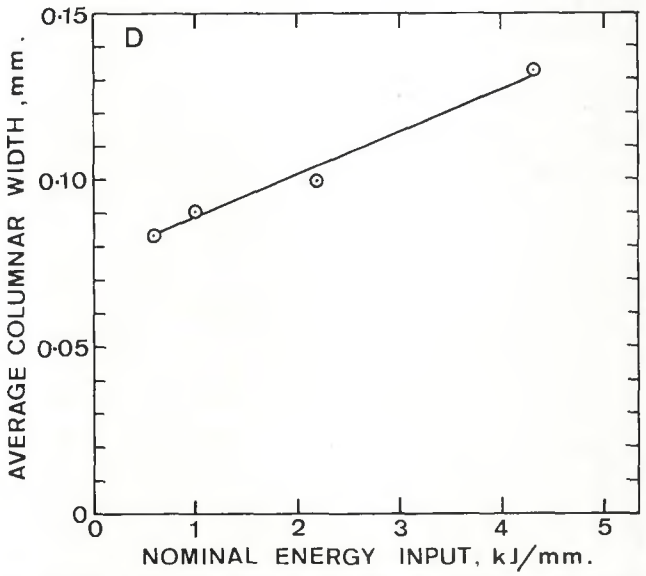

Fig. 7 — Effect of heat input on the average columnar grain width (electrode D)

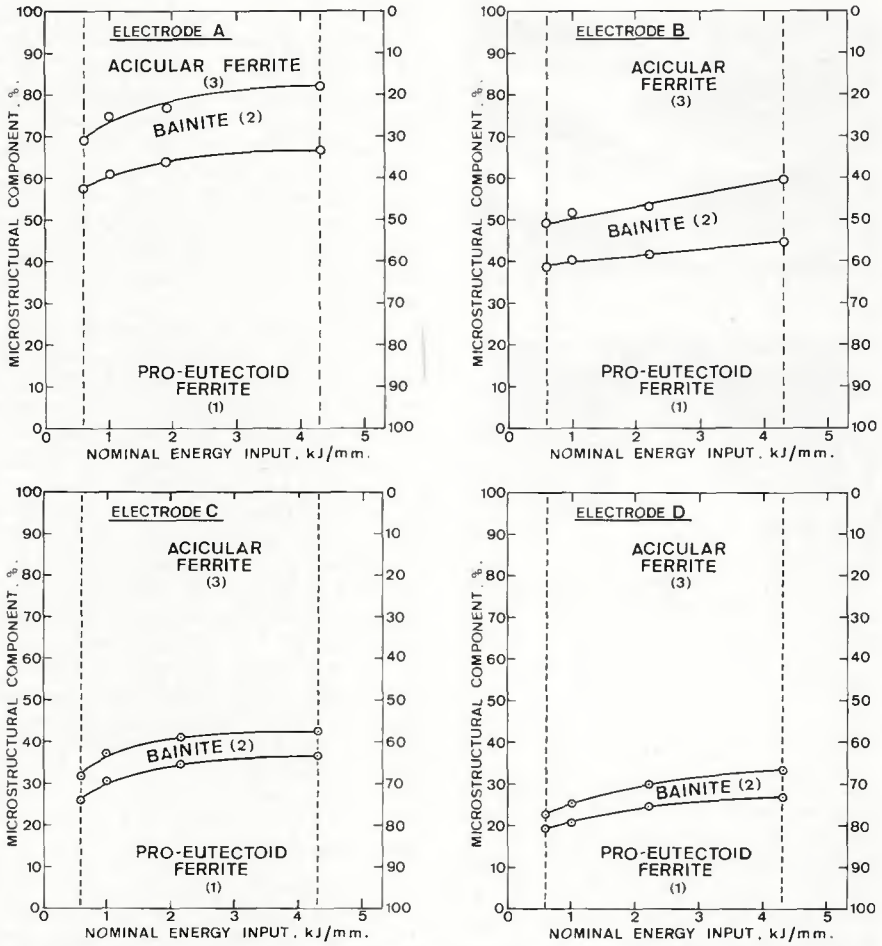

Fig. 8—Effect of heat input on the microstructure of as-deposited weld metal (different Mn levels)

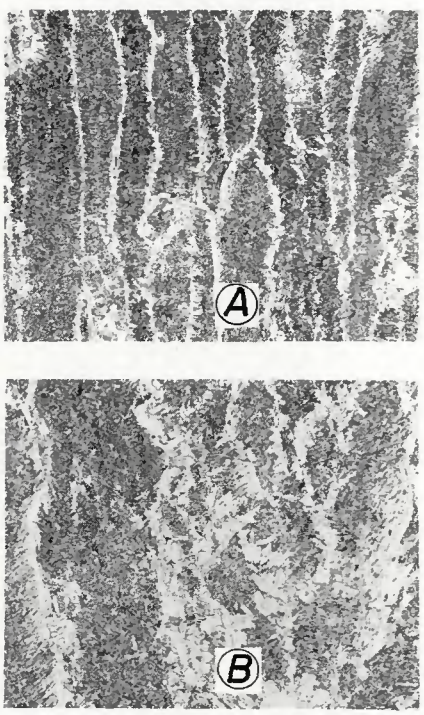

Fig. 9—Photomicrographs of top beads (columnar): A—C, 0.6 kJ/mm; B—4.3 kJ/mm. X100 (reduced 37% on reproduction)

following regressions were obtained:

- For yield strength (in N/mm2):

0.6 kJ/mm
Y.S. = 376 + 105 Mn ..... (1)
1.0 kJ/mm
Y.S. = 352 + 88 Mn ..... (2)
2.2 kJ/mm
Y.S. = 351 + 62 Mn ..... (3)
4.3 kJ/mm
Y.S. = 301 + 78 Mn ..... (4)

- For ultimate tensile strength (in N/mm2):

0.6 kJ/mm
U.T.S. = 428 + 105 Mn ..... (5)
1.0 kJ/mm
U.T.S. = 406 + 102 Mn ..... (6)
2.2 kJ/mm
U.T.S. = 410 + 80 Mn ..... (7)
4.3 kJ/mm
U.T.S. = 417 + 68 Mn ..... (8).

In general, manganese had a progressively weaker strengthening effect as the heat input was increased; the tensile parameter change (for a 0.1% increment in Mn) was approximately 10 N/mm2 and 7 N/mm2 for the two extremes of energy input investigated.

Impact Results. The Charpy-V transition curves obtained are presented in Fig. 17. The trends for specific test temperatures are drawn in Fig. 18, as functions of manganese content, and show peak distributions of the form observed previously (Ref. 1-3).

The effect of heat input on the lateral shift of the transition curves is depicted in Fig. 19 by plotting the Charpy-V temperatures required to give absorbed energy

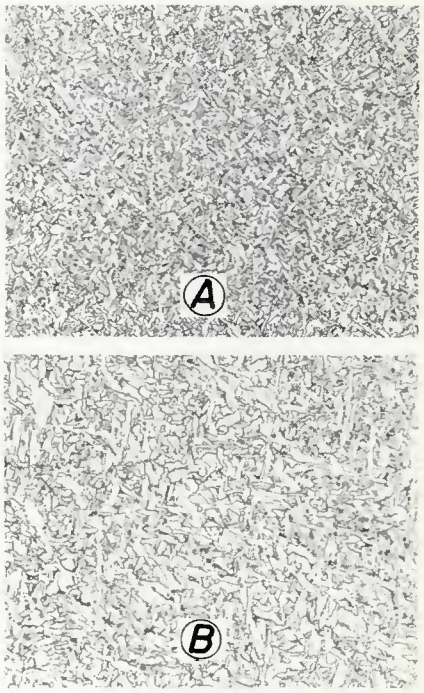

Fig. 10—Photomicrographs of acicular ferrite in columnar regions: A—C, 0.6 kJ/mm; B—4.3 kJ/mm. X630 (reduced 37% on reproduction)

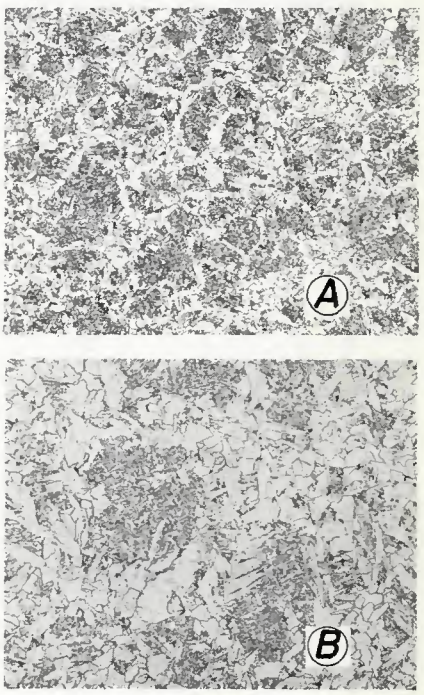

Fig. 11—Photomicrographs of coarse grained regions (electrode C): A—0.6 kJ/mm; B—4.3 kJ/mm. X200 (reduced 37% on reproduction)

Table 3—Hardness of As-Deposited Metal

Heat input, kJ/mm	Hardness, HV 5			
	A	B	C	D
0.6	176	191	223	233
1.0	169	183	215	226
2.2	171	178	203	228
4.3	155	175	184	208

values of 100 J and 28 J. It is seen that optimum impact properties were attained at approximately 2 kJ/mm. The same results are reconsidered in Fig. 20 and reveal that the optimum with regard to manganese content occurred at about 1.4% Mn.

Discussion

A variation in heat input (achieved by varying the run out length of the electrodes) led automatically to a variation in bead size. This, in turn, led to different numbers of beads per layer and finally, on completion of the welds, to different numbers of layers. The build-up sequences were such as to produce totally dissimilar conditions with regard to overlapping in the central parts of the deposits. The situation was hence more complex than in previous work where the number of beads per layer had been standardized and where the extent of recrystallization was systematically modified by varying the interpass temperature (Ref. 2) and the electrode diameter (Ref. 3).

Metallographic studies revealed that the structure of as-deposited weld metal changed as heat input was increased. On a macroscale, the increased bead size was accompanied by an increase in the width of the columnar grains; on a microscale, the amount of pro-eutectoid ferrite was found to increase at the expense of the acicular ferrite. The latter effect was limited when considered on a percentage basis. However, the ferrite veins became wider as a consequence of fewer sites being available for nucleation. Furthermore, the acicular ferrite per se became progressively coarser as a result of retarded cooling rates leading to transformation occurring over higher temperature ranges. The reheated regions were also adversely affected, grain growth taking place in both the coarse and the fine grained zones as the speed of welding was reduced.

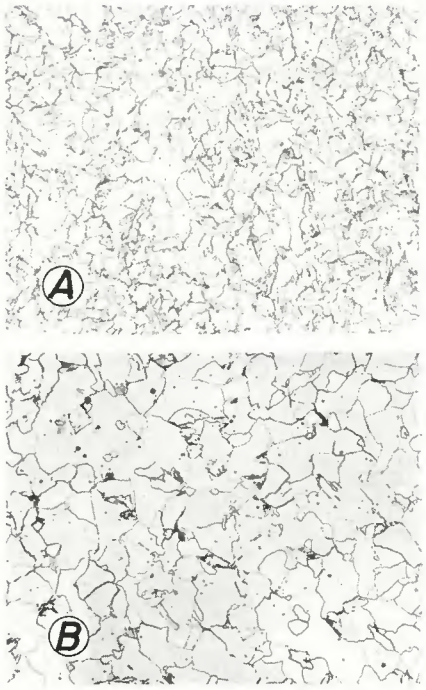

Fig. 12—Photomicrographs of fine grained regions (electrode C): A—0.6 kJ/mm; B—4.3 kJ/mm. X630 (reduced 37% on reproduction)

Yield and tensile strengths decreased as the heat input was increased. In addition, the strengthening effect of manganese was influenced, the slope of the lines in Fig. 16 decreased as the run-out length was reduced. The situation over the tensile cross-sections differed to such an extent that, in contrast to previous work (Ref. 2, 3), non-linear relationships

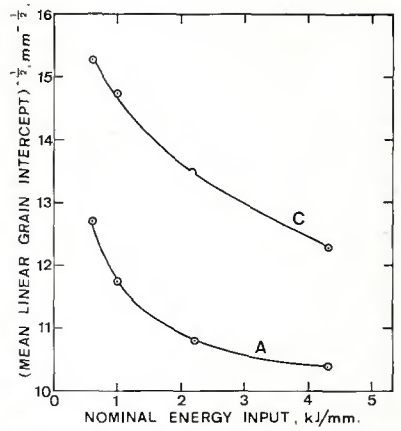

Fig. 13—Effect of heat input on the grain intercept in the fine grained region (deposits A and C)

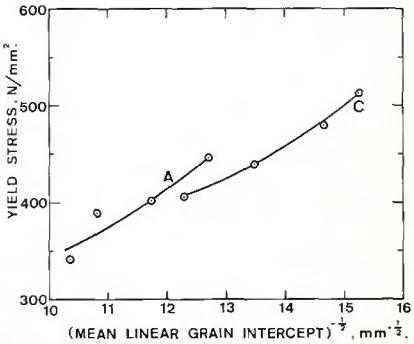

Fig. 14—Plot of yield stress against the grain intercept in the fine grained region (deposits A and C)

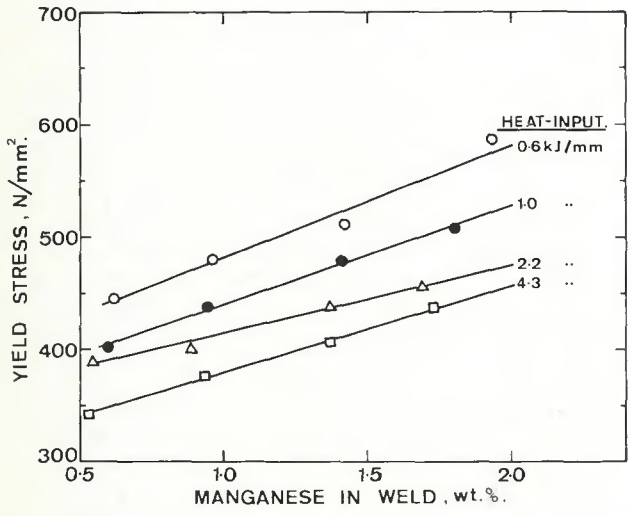

Fig. 15—Effect of manganese on yield stress (different heat inputs)

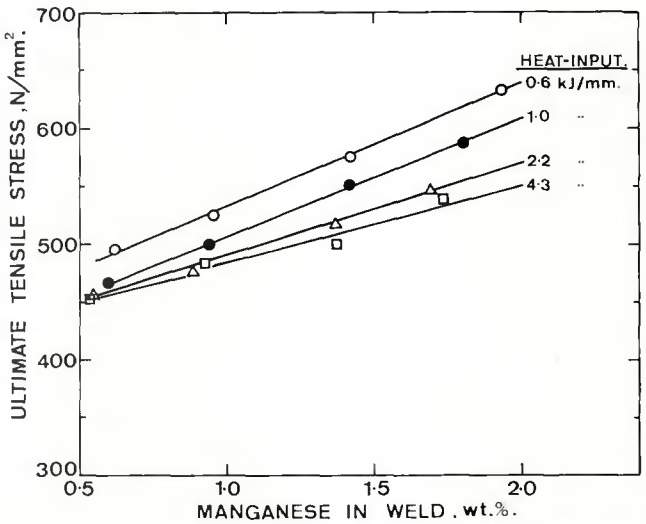

Fig. 16—Effect of manganese on ultimate tensile stress (different heat inputs)

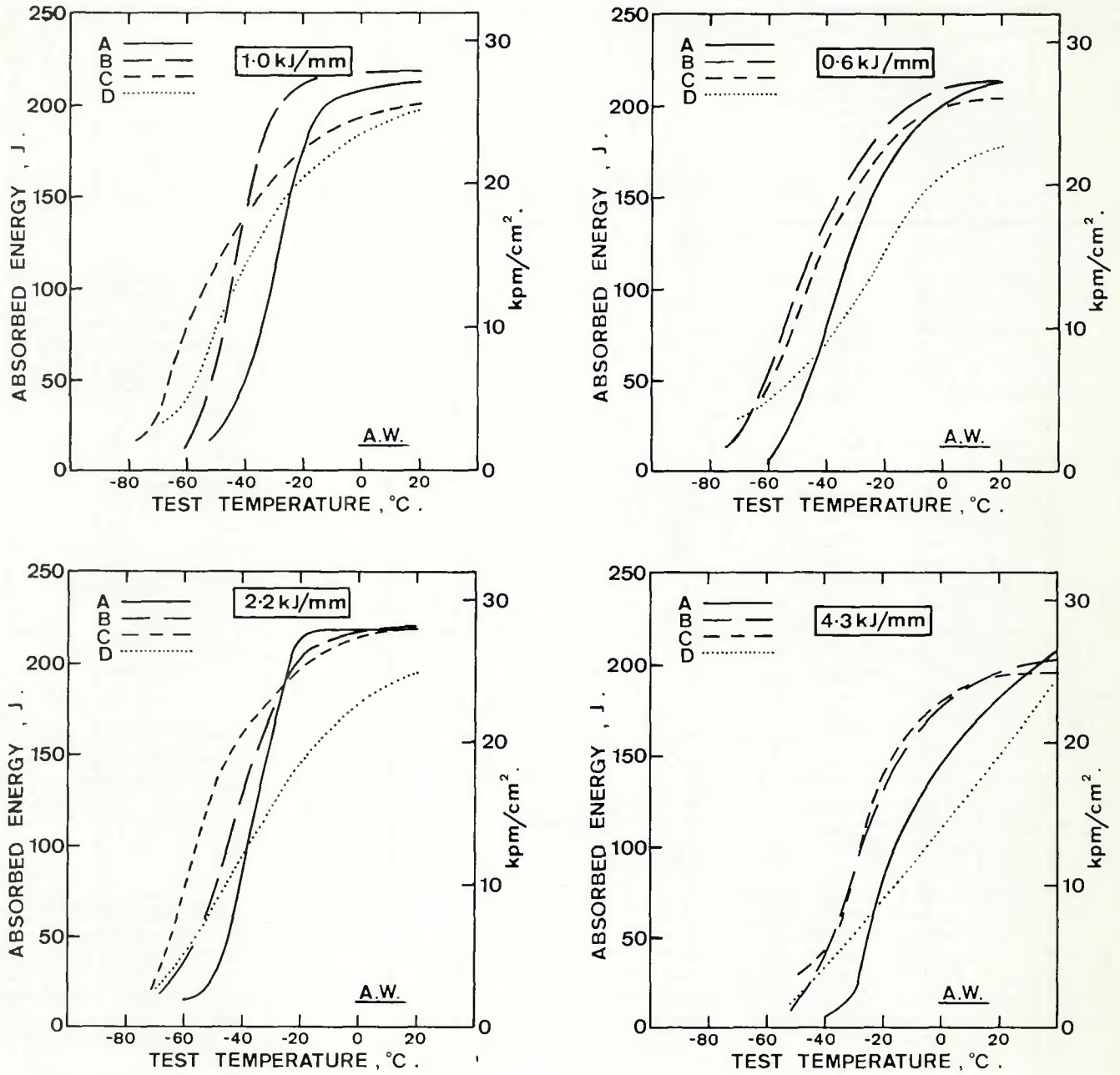

Fig. 17 – Charpy V-notch impact test results

Table 4—Effect of Notch Location

Beads/ layer	Heat input, kJ/mm	Electrode	Temp. °C[a] at 100 J		Difference[b] °C
			Center	Displaced	
3	1.0	A	−31	−50	−19
		B	−46	−66	−20
		C	−54	−63	− 9
		D	−44	−56	−12
2	2.2	A	−39	−24	+15
		B	−46	−30	+16
		C	−57	−46	+11
		D	−38	−37	+ 1

(a) °F = 9/5 °C + 32
(b) °F = 1.8 × °C

were found between the yield stress and the grain size factor. Also, precipitation hardening took place on repeated cycling, the minimum hardness occurring directly below the last bead to be deposited.

Charpy-V test results revealed that optimum toughness was generally attained when two beads per layer were deposited. The notch, in this case, was located in an overlap region where complete recrystallization had taken place (Fig. 4). The situation thus differed from that occurring for a lower heat input weld having three beads per layer. In the latter instance, approximately 25% columnar weld metal remained at the notch location, the overlap regions being located approximately 3 mm (0.12 in.) on either side of the centre line (Fig. 5).

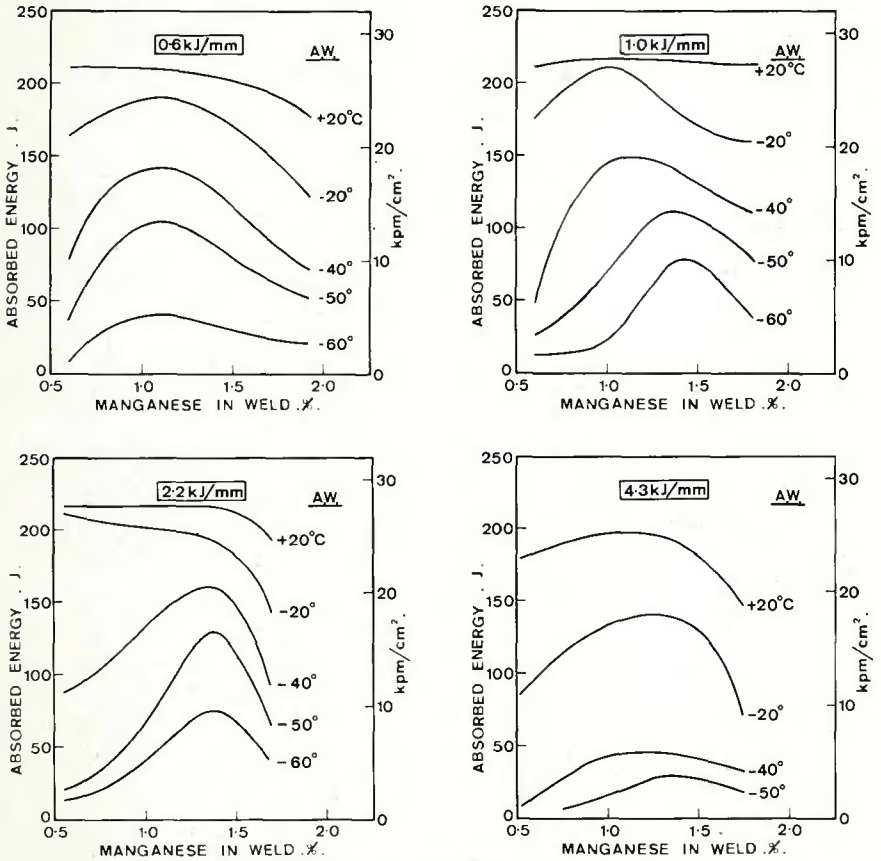

Fig. 18—Effect of manganese on energy absorbed (different heat inputs)

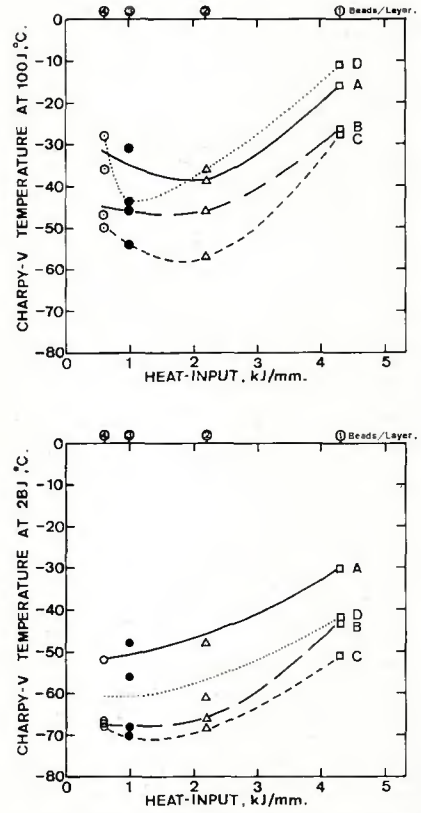

Fig. 19—Effect of heat input on Charpy V test temperature corresponding to 100 J and 28 J (different Mn levels)

Additional Charpy-V data obtained for the notch displaced by this distance are included in Table 4 for deposits having 3 and 2 beads per layer.

Displacement was beneficial for 1 kJ/mm, the lateral shift at an arbitrary level of 100 J being to lower temperatures. The converse occurred for the two bead per layer deposits. Comparison of the equivalent fully recrystallized regions reveals the lower heat input condition to be the better. Thus, when a joint is considered "in toto," it follows that a normal stringer bead sequence is preferable to a limited weave technique. A too rapid rate of travel, however, is not recommended, since greater amounts of silicon and possibly oxygen are retained. At the other extreme, grain coarsening is such in a fully weaved deposit that poorer impact properties are a natural consequence.

The present data are applicable to a specific low hydrogen iron powder electrode. It could well be that different trends would be exhibited for low alloy steel electrodes or for electrodes of another slag base type. Furthermore, all test plates were prepared in the horizontal position; it now remains to make a comparison with limited and fully weaved deposits welded vertically up. An interesting feature of the present work, however, was that the optimum composition with regard to impact properties was still maintained at approximate-

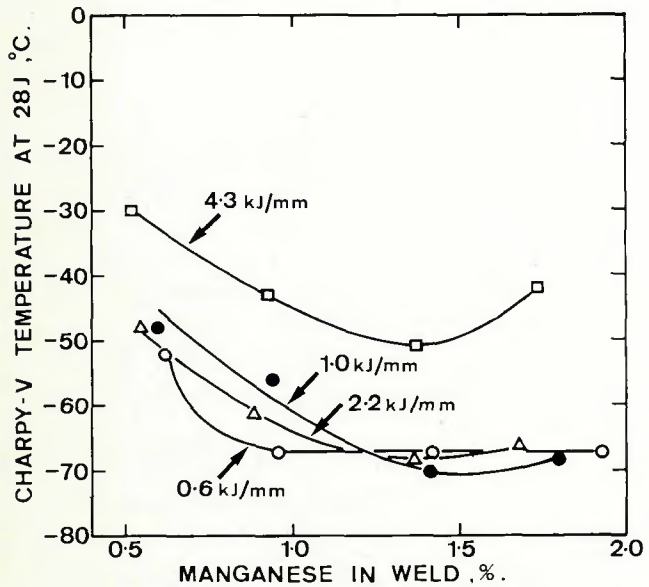

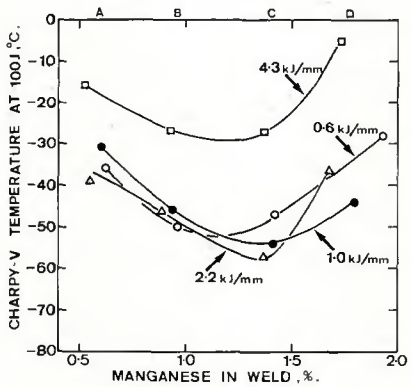

Fig. 20—Effect of manganese on Charpy-V test temperature corresponding to 100 J and 28 J (different heat inputs)

ly 1.4% manganese, independently of heat input.

Conclusion

For ISO 2560 type deposits, welded with basic iron powder electrodes of a specific slag base type, the following occurred as a result of increasing the heat input:

1. The weld metal manganese and silicon contents were reduced.
2. The number of beads per layer varied, and the nugget and recrystallized areas increased.
3. The hardness of as-deposited weld metal decreased.
4. The average width of the columnar grains increased.
5. The amount of pro-eutectoid ferrite in as-deposited weld metal increased at the expense of the acicular ferrite.
6. The lath size of the acicular ferrite increased.
7. The microstructure of the high temperature reheated regions coarsened, the width of the ferrite envelopes increasing.
8. The grain size of the equiaxed fine grained regions increased.
9. The amount of columnar weld metal remaining in the bulk of the deposit varied.
10. The yield strength and the tensile strength decreased.
11. The strengthening effect of manganese decreased.
12. Optimum Charpy-V impact properties were achieved at 2 kJ/mm, when the notch was centrally located.
13. Better impact properties were achieved at 1 kJ/mm when the notch was displaced away from the center line.
14. The optimum manganese level with regard to impact properties remained at approximately 1.4%.

References

1. Evans, G. M. 1977. *Effect of manganese on the microstructure and properties of C-Mn all-weld metal deposits.* IIW doc. II-A-432-77.

2. Evans, G. M. 1978. *Effect of interpass temperature on the microstructure and properties of C-Mn all-weld metal deposits.* IIW doc. II-A-460-78.

3. Evans, G. M. 1979. *Effect of electrode diameter on the microstructure and properties of C-Mn all-weld metal deposits.* IIW doc. II-A-469-79.

4. Davey, T. G., and Widgery, D. J. 1976. *A technique for the characterisation of weld metal microstructures.* IIW doc II-A-389-76.

5. Results of a joint international study: 1979. *The quantification of weld metal microstructures.* IIW doc. II-A-479-79 (II-899-79).

WRC Bulletin 270
September, 1981

Long-Range Plan for Pressure Vessel Research—Sixth Edition
by The Pressure Vessel Research Committee

Every three years, the PVRC Long-Range Plan is reissued. The Fifth Edition was distributed as widely as possible for review and comment. A number of additional problem areas have been suggested by the ASME BPVC, as well as by other organizations and by individuals within PVRC. Most of the problems in the Fifth Edition have been modified to meet current needs, and a number of new problems have been added to this Sixth Edition.

The list of "PVRC Research Problems" is comprised of 64 research topics, divided into three groups relating to the three divisions of PVRC—*i.e.*, Materials, Design and Fabrication. Each project is outlined briefly in a project description, giving the Title, Statement of Problem and Objectives, Current Status, and Action Proposed.

Because of budget limitations, PVRC will not be able to investigate all of these problems in the foreseeable future. Therefore, the cooperation and efforts of other groups in studying these areas is also invited. If work is planned on one of the problems, PVRC should be informed in order to avoid duplication.

Publication of this bulletin was sponsored by the Pressure Vessel Research Committee of the Welding Research Council.

The price of WRC Bulletin 270 is $11.50 per copy. Orders should be sent with payment to the Welding Research Council, 345 East 47th St., New York, NY 10017.

WRC Bulletin 274
January, 1982

International Benchmark Project on Simplified Methods for Elevated Temperature Design and Analysis: Problem II—The Saclay Fluctuating Sodium Level Experiment; Comparison of Analytical and Experimental Results; Problem III—The Oak Ridge Nozzle to Sphere Attachment
by H. Kraus

Problem II. Recently, experimental results became available on the second benchmark problem on simplified methods for elevated temperature design and analysis: the Saclay fluctuating sodium level experiment. These are compared to previously published numerical and analytical results in WRC Bulletin 258, May 1980.

Problem III. The Oak Ridge Nozzle to Sphere Attachment is analyzed by finite element computer programs and by approximate analytical techniques. The methods are described and the results obtained by each are compared. No experimental data are available.

Publication of these reports was sponsored by the Subcommittee on Elevated Temperature Design of the Pressure Vessel Research Committee of the Welding Research Council.

The price of WRC Bulletin 274 is $10 per copy, plus $3.00 for postage and handling. Orders should be sent with payment to the Welding Research Council, 345 East 47th St., New York, NY 10017.